Applied Catalysis B: Environmental 90 (2009) 545–555

Contents lists available at ScienceDirect

Applied Catalysis B: Environmental

journal homepage: www.elsevier.com/locate/apcatb

Catalytic behaviour of thermally aged Ce/Zr mixed oxides for the purification of chlorinated VOC-containing gas streams

Beatriz de Rivas, Rubén López-Fonseca, Carmen Sampedro, José I. Gutiérrez-Ortiz *

Chemical Technologies for Environmental Sustainability Group, Department of Chemical Engineering, Faculty of Science and Technology, Universidad del País Vasco/EHU, P.O. Box 644, E-48080 Bilbao, Spain

ARTICLE INFO

Article history:
Received 22 December 2008
Received in revised form 3 April 2009
Accepted 9 April 2009
Available online 21 April 2009

Keywords:
Chlorinated VOCs
Catalytic combustion
Ceria–zirconia mixed oxides
Thermal aging
Sintering

ABSTRACT

In the present paper the thermal deactivation of a series of Ce/Zr mixed oxides (CeO_2, $Ce_{0.8}Zr_{0.2}O_2$, $Ce_{0.68}Zr_{0.32}O_2$, $Ce_{0.5}Zr_{0.5}O_2$, $Ce_{0.15}Zr_{0.85}O_2$ and ZrO_2) was investigated. In order to simulate long-term operation, samples were calcined at three different temperatures, namely 550, 750 and 1000 °C in air for 4 h. Structural, morphological and physico-chemical changes caused by high-temperature treatment were analysed by X-ray diffraction, BET measurements, NH_3-temperature-programmed desorption and temperature-programmed reduction with hydrogen, and the behaviour in the oxidation of chlorinated volatile organic compounds (1,2-dichloroethane and trichloroethylene). The catalytic properties of Ce/Zr mixed oxides could be accounted for on the basis of their promoted redox, as characterised by the percentage of oxygen vacancies, and acidic properties due to the incorporation of zirconium in the ceria lattice. An increase in the calcination temperature led to a progressive decrease in the catalytic activity as a result of the modifications provoked by induced thermal aging (decrease in surface area, larger crystal sizes, reducibility at higher temperatures and loss of acid sites). $Ce_{0.15}Zr_{0.85}O_2$ and $Ce_{0.5}Zr_{0.5}O_2$ showed the best resistance to deactivation with combustion temperatures still notably lower in comparison with the homogeneous reaction even after calcination at 1000 °C. Also slight changes in selectivity were evident resulting in favoured yields of hydrogen chloride, which was environmentally beneficial, and incomplete combustion products such as carbon monoxide and chlorinated intermediates.

1. Introduction

Chlorinated volatile organic compounds (Cl-VOCs) are common industrial solvents and by-products from the manufacture of chlorinated chemicals such as plastics [1]. These environmentally hazardous compounds are often carcinogens and mutagens and may deplete stratospheric ozone. However, since for a variety of applications, chlorinated hydrocarbons are still indispensable, techniques to avoid or reduce emissions of these compounds have to be developed [2]. Most toxic chlorinated compounds released from industrial and commercial sources are chlorinated alkanes and alkenes that contain between one and three carbon atoms. Environmental legislation in the USA and the EU is indeed posing increasingly stringent standards on VOC emissions, the satisfaction of which requires significant improvement in the efficiency of removal technologies. Also public and corporate pressure and the drive towards clean technology in the chemical industry have attracted considerable concerns on emissions control of this type of VOCs.

When the recovery of these compounds is not desired or economically feasible catalytic abatement for Cl-VOC-containing waste gases (i.e., total oxidation of trace amounts in air-rich gas streams) is one of the most important air pollution control techniques. The most relevant application of this strategy refers to treatment of off-gases from chemical plants, groundwater decontamination by air stripping followed by oxidation, odour emission control, and treatment of contaminated air in solvent evaporation processes. Apart from a relatively low cost, a suitable catalyst for this application in environmental remediation should fulfil several strict requirements. The catalyst must show high activity at low temperatures for the destruction for a diverse range of Cl-VOCs to carbon oxides (preferably to carbon dioxide). Additionally it must produce high selectivity to HCl for the prevention of secondary environmental pollution. The catalyst should also show flexibility to changes in operating conditions (for example, the presence of water), and be able to treat effluents containing VOC mixtures. And, last but not least, the catalyst must exhibit an adequate thermal and chemical stability with a remarkable resistance to deactivation. An adequate balance between the catalytic activity and selectivity and its long-term durability is indeed crucial. All these factors are binding on the commercial application of the catalyst in industrial processes, and

* Corresponding author. Tel.: +34 94 6012683; fax: +34 94 6015963.
E-mail address: joseignacio.gutierrez@ehu.es (Gutiérrez-Ortiz).

0926-3373/$ – see front matter © 2009 Published by Elsevier B.V.
doi:10.1016/j.apcatb.2009.04.017

have consequently spurred considerable interest in search of suitable materials. Most research in this area focuses on known oxidation catalysts, such as supported noble metals and metal oxides [3–5], and solid acid catalysts, such as zeolites [6–9]. As an alternative the use of bulk mixed oxides, which combine both catalytic properties, has been recently proposed. Perovskites, and manganese–zirconia and ceria–zirconia solid solutions can be included in this third class of VOC catalysts [10–12].

Numerous studies have recently led to a significant understanding of the process of Cl-VOC catalyst deactivation, mainly, by chlorine-poisoning (also sulphur-, lead-, silicon- or phosphorous-poisoning) or coking [13–17]. These studies have been carried out for noble or transition metal catalysts. The most serious drawback is related to the volatility of some of metal (oxy)chlorides which can be formed during reaction leading to the loss of the catalytic agent. Their formation and elution will shorten the lifetime of the catalyst and noticeably limit their applicability. As a result, application of metal-based catalysts is restricted to low operation temperatures.

Ce/Zr mixed oxides have recently gained increased interest in several environmental applications. Apart from its widely known excellent performance as three-way catalysts for the treatment of exhaust gases in gasoline automobile converters [18,19], the unique features of oxygen storage capacity have made these systems important in other catalytic processes including CO oxidation [20], light hydrocarbons combustion [21], VOC oxidation [22], and soot removal [23]. In the course of our recent work, we have reported the high activity and selectivity of Ce/Zr mixed oxides for oxidation of Cl-VOCs [24–26]. In these studies it was evidenced that this type of catalysts do not favour the formation of coke deposits, which is a major factor known to occur to aluminosilicates (protonic zeolites), thereby inhibiting the eventual deactivation by this phenomenon. Note that, apart from the catalyst itself, the type of chlorinated feed used also appears to be a major factor in influencing the extent of deactivation by coking (hydrogen-rich chlorinated compounds, for example 1,2-dichloroethane or chloropropanes, and chlorinated aromatics, exhibit propensity to form coke [27–30]). Further, the impact of chlorination of Ce/Zr catalysts was observed to be limited resulting in a slight loss of activity [31].

In further pursuance of our catalytic studies with Cl-VOCs over Ce/Zr mixed oxides, several thermally aged (at 750 and 1000 °C) mixed oxides were investigated for their catalytic behaviour during vapour-phase oxidation of two different double carbon feeds, namely 1,2-dichloroethane (DCE) and trichloroethylene (TCE), as model reactions for the catalytic combustion of chlorinated organic pollutants. These compounds were selected on account of their different ease of destruction (high for DCE and low for TCE) and hydrogen balance, and may actually provide some representative information of the ability of these mixed oxides to decompose other Cl-VOCs.

2. Experimental

2.1. Catalyst preparation

Four ceria–zirconia mixed oxides with varying Ce/Zr ratio were synthesised by Rhodia using a precipitation route from nitrate precursors. Rhodia also provided the pure ceria sample whereas the pure zirconia sample was supplied from Norton. Samples were labelled as CZ XX/YY-T where XX, YY and T are the Ce %molar content, the Zr %molar content, and the calcination temperature, respectively. The molar Ce loading of the samples was: 0, 15, 50, 68, 80 and 100%. Pure and mixed oxides were stabilised by calcination in air at 550 °C for 4 h in a muffle furnace (fresh samples). Thermally aged oxides were prepared by calcination at 750 and 1000 °C for 4 h in air. Catalyst pellets with diameter from 0.3 to 0.5 mm were prepared by compressing the oxide powders into flakes in a hydraulic press (2.2×10^5 kPa, Specac), followed by crushing and sieving. Fresh and aged catalysts, and before they were subjected to catalytic activity and selectivity experiments, were characterised using several analytical techniques.

2.2. Characterisation techniques

Textural properties were evaluated from the nitrogen adsorption–desorption isotherms, determined at −196 °C with a Micromeritics ASAP 2010 apparatus. The specific areas of the samples were determined according to the standard BET procedure using nitrogen adsorption taken in the relative equilibrium pressure interval of 0.03–0.3. Mean pore size was calculated from the BJH method. The samples were previously degassed overnight at 300 °C under high vacuum. X-ray diffraction (XRD) studies were carried out on a X'PERT-MPD X-ray diffractometer with Cu Kα radiation (λ = 1.5406 Å) and Ni filter. The X-ray tube was operated at 30 kV and 20 mA. Samples were scanned from $2^\circ < 2\theta < 80^\circ$ and the X-ray diffraction line positions were determined with a step size of 0.02° and a counting time of 2.5 s per step. Indexation and calculation of unit cell parameters were carried out by using the intensities of lines (1 1 1) of CZ 100/0, CZ 80/20 and CZ 68/32 (cubic structure), (1 0 1) of CZ 50/50 and CZ 15/85 and (1 1 1) and (1 0 1) of CZ 0/100 (tetragonal and monoclinic structure, respectively). Phase identification was carried out by comparison with JCPDF database cards.

Temperature-programmed desorption (TPD) of ammonia was performed on a Micromeritics AutoChem 2920 instrument equipped with a quartz U-tube coupled to a thermal conductivity detector. Prior to adsorption experiments, the samples (30 mg) were first pre-treated in a 5%O_2/He stream at 550 °C. Then, they were cooled down at 100 °C in a He flow (20 cm^3 min^{-1}). Later, the NH_3 adsorption step was performed by admitting a flow of 10%NH_3/He at 100 °C up to saturation. Subsequently, the samples were exposed to a flow of helium (50 cm^3 min^{-1}) for 2 h at 100 °C in order to remove reversibly and physically bound ammonia from the surface. Finally, desorption was carried out from 100 to 550 °C at a heating rate of 10 °C min^{-1} in an He stream (50 cm^3 min^{-1}). This temperature was maintained for 120 min until the adsorbate was completely desorbed. The amount of gases desorbed was determined by time integration of the TPD curves.

The redox behaviour was examined by temperature-programmed reduction experiments (TPR). These experiments were conducted on a Micromeritics AutoChem 2920 instrument as well. Firstly, all the samples were pre-treated in an oxygen stream (5%O_2/He) at 550 °C for 1 h, and then cooled down to room temperature. The reducing gas used in all experiments was 5%H_2 in Ar, with a flow rate of 50 cm^3 min^{-1}. The temperature range explored was from room temperature to 950 °C with a heating rate of 10 °C min^{-1}. This temperature was maintained for 30 min so as to complete the reduction process. The water produced by reduction was trapped into a cold trap. The consumption of H_2 was quantitatively measured by time integration of the TPR profiles.

2.3. Catalyst activity determination

Catalyst behaviour was determined using a lab-scale fixed-bed reactor, in which typically 0.85 g of catalyst was loaded. Catalysts were tested in powdered form (0.3–0.5 mm) using a 12-mm i.d. stainless-steel reactor tube [32]. The catalysts were secured in the reactor tube by plugs of silica wool. The reaction feed consisted of 1000 ppm of each Cl-VOC examined in dry air. The feed stream to the reactor was prepared by delivering each liquid hydrocarbon by

a syringe pump (KDS 100) into dry air, which was metered by a mass flow controller (Brooks). Mass flow controllers were used to control the flow rates of gases to the reactor, and a liquid vaporisation system was employed to create the air stream containing chlorinated VOCs. A total flow rate of 500 $cm^3\ min^{-1}$ was used and catalysts were packed to a constant volume to give a gas hourly space velocity of 30,000 h^{-1} for all studies. Catalytic activity was examined over the range 200–550 °C, and temperatures were measured by a thermocouple placed in the catalyst bed. Assuming that the flow rate at the inlet and the outlet of the reactor was identical (due the large excess of oxidant used), VOC conversion data were calculated by the difference between inlet and outlet concentrations according to the following equation:

$$\text{conversion}\,(\%) = \frac{C_{\text{inlet}} - C_{\text{outlet}}}{C_{\text{inlet}}} \times 100 \quad (1)$$

Conversion measurements and product profiles were taken at steady state, typically after 30 min on stream. Either product selectivity was calculated based on either chlorine or carbon atoms present in that product divided by the total chlorine or carbon atoms present in the product stream (expressed as %). The feed and effluent streams were analysed using an on-line 7980A Agilent Technologies gas chromatograph equipped with a thermal conductivity (CO and CO_2) and an electron capture detector (chlorinated hydrocarbons). Analysis of HCl and Cl_2 was carried out by means of ion selective electrode and titration, respectively. Further details on analytical procedures are described elsewhere [32].

3. Results

3.1. Characterisation of fresh and thermally aged Ce/Zr samples

The evolution of the textural properties as a function of the calcination temperature in terms of specific surface area, pore volume and average pore size is shown in Table 1. As for fresh samples it was found that all oxides showed a surface area of around 100 $m^2\ g^{-1}$, except for CZ 15/85-550 (85 $m^2\ g^{-1}$) and CZ 0/100-550 (50 $m^2\ g^{-1}$). These samples had substantially higher surface area than the thermally aged counterparts. Hence, after calcination at 750 °C a remarkable loss was noticed which varied from 45 to 70%. These results also suggested that the addition of relatively large amounts of zirconium atoms (>32 mol%) enhanced the thermal stability of the mixed oxides. Aging at 1000 °C resulted in a more dramatic impact on the sintering of the samples with values as low as 10–18 $m^2\ g^{-1}$ depending on the sample considered [33]. Under these conditions the beneficial effect of zirconium atoms was found to be minimised. All the adsorption/desorption isotherms of fresh samples corresponded to mesoporous materials (type IV isotherms according to BDDT classification). Aged mixed oxides also presented isotherms of type IV, but in this case the hysteresis loops were significantly reduced. This indicated a gradual reduction of the pores system, essentially due to the destruction of the smaller pores, with the thermal treatment, and a subsequent increase in the average size of the remaining pores as revealed by the BJH pore size distribution (not shown). Finally, it is worth pointing out that no trend was observed between the Ce/Zr ratio and the pore volume whatever the calcination temperature.

The XRD patterns of the samples calcined at 550 °C (Fig. 1) presented broad reflections due to a poor crystallinity and small particle size. Even so, the main reflections corresponding to the cubic structure of ceria could be clearly observed for Ce-rich compositions (CZ 100/0-550, CZ 80/20-550 and CZ 68/32-550). In contrast, the CZ 50/50-550 and CZ 15/85-550 oxides showed the reflections associated with the tetragonal phase. However, the pattern of CZ 15/85-550 included peaks attributable to monoclinic zirconia as well. This revealed a partial lack of insertion of the zirconia into the solid solution. On the other hand, the structure of the pure zirconia (CZ 0/100-550) was monoclinic. All the samples could be therefore considered as homogeneous solid solutions, except for CZ 15/85-550.

At higher calcination temperatures more intense well-resolved reflections were typically noticeable in agreement with concomitant gradually lower surface areas and larger particle sizes (higher crystallinity), as shown in Fig. 1 and Table 1. This effect resulted more relevant for the samples calcined at 1000 °C. The influence of the thermal treatment on the crystal size growth in CZ 100/0-550 was considerable larger than in any of the Ce/Zr mixed oxides [34,35]. This indicated that the dissolution of zirconium ions into the ceria lattice depressed the crystal size growth. This increase in the particle size corresponded fairly well to the decrease in the surface area.

Nevertheless, the aging treatment did not affect all Ce/Zr samples in the same way. It is important to note the relatively low value of the particle size for CZ 50/50-550, which practically remained unaltered irrespective of the calcination temperature. According to the literature and taking the phase diagram into account [36], it was expected that this equimolar sample would be the most easily segregated composition. Thus, if the diffraction

Table 1
Textural and structural properties of the Ce/Zr mixed oxides as a function of the calcination temperature.

Catalyst	BET surface area ($m^2\ g^{-1}$)	Pore volume ($cm^3\ g^{-1}$)	Average pore size (Å)	Structure	Crystal size (nm)
CZ 100/0-550	99	0.21	59	c-CeO_2	9.9
CZ 80/20-550	102	0.18	48	c-CeO_2	6.9
CZ 68/32-550	101	0.24	70	c-CeO_2	7.8
CZ 50/50-550	99	0.21	64	t-CeO_2	7.0
CZ 15/85-550	86	0.28	102	t-CeO_2 + m-ZrO_2	6.4
CZ 0/100-550	51	0.25	157	m-ZrO_2	14.5
CZ 100/0-750	59	0.18	123	c-CeO_2	11.9
CZ 80/20-750	53	0.13	94	c-CeO_2	10.5
CZ 68/32-750	62	0.20	129	c-CeO_2	9.5
CZ 50/50-750	67	0.18	110	t-CeO_2	7.1
CZ 15/85-750	60	0.23	156	t-CeO_2 + m-ZrO_2	9.0
CZ 0/100-750	26	0.13	197	m-ZrO_2	17.6
CZ 100/0-1000	18	0.13	219	c-CeO_2	37.0
CZ 80/20-1000	11	0.08	223	c-CeO_2	24.6
CZ 68/32-1000	17	0.13	247	c-CeO_2	15.1
CZ 50/50-1000	15	0.09	209	t-CeO_2	7.7
CZ 15/85-1000	17	0.11	233	t-CeO_2	23.8
CZ 0/100-1000	10	0.07	279	m-ZrO_2	31.9

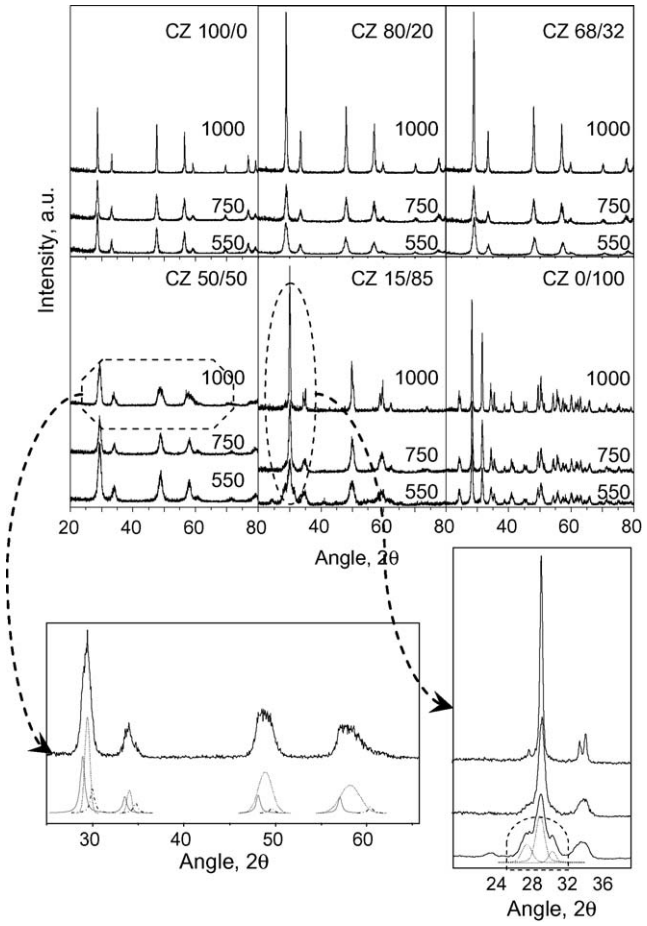

Fig. 1. XRD diffraction patterns of the Ce/Zr mixed oxides as a function of the calcination temperature.

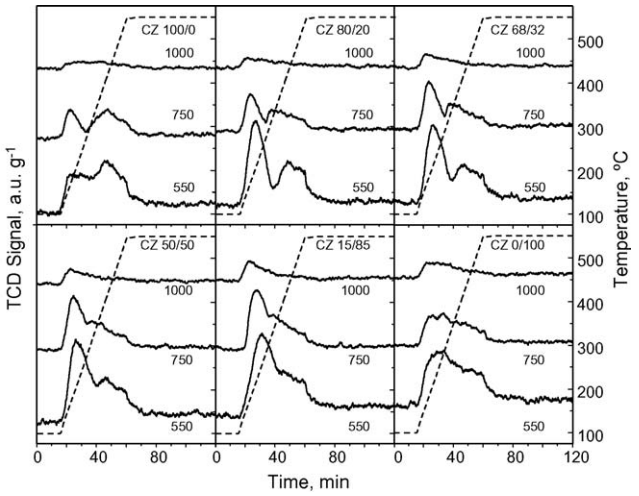

Fig. 2. NH_3-TPD profiles of the Ce/Zr mixed oxides as a function of the calcination temperature.

pattern of this oxide calcined at 1000 °C were more thoroughly examined, the appearance of asymmetric peaks could be distinctly noticed (Fig. 1). This feature was attributed to the metastable nature of this mixed oxide, leading to a partial phase segregation into more stable compositions at high temperatures [33]. The new phases that appeared gradually upon calcination corresponded to phases whose compositions were approximately cubic 80 mol% Ce/20 mol% Zr and tetragonal 20 mol% Ce/80 mol% Zr [37]. This could explain the fact that the crystal size remained virtually constant whereas the surface area decreased. It must be noted that the crystal size was calculated on basis of the XRD data for the 50 mol% Ce/50 mol% Zr composition but the surface area corresponded to the whole mixture of $(Ce,Zr)O_2$ phases present in the mixed oxide. Yao-Matsuo et al. [38] also reported that Ce/Zr solid solutions with a Ce molar composition of 50 mol% presented segregation into two other phases after hydrothermal treatment. Except for this specific mixed oxide no indication of phase splitting or de-mixing was detected for the other mixed oxides. Finally, it is also worth pointing out that most of zirconia previously detected in CZ 15/85-550 was incorporated into the lattice upon calcination at higher temperatures since diffraction peaks assigned to monoclinic zirconia were no longer detected.

Another major difference between fresh and aged catalysts was the total acidity. NH_3-TPD profiles for all Ce/Zr oxides, normalised to the mass of the catalyst, are shown in Fig. 2. The total amount of desorbed ammonia, expressed as μmol of adsorbed NH_3 per gram of catalyst and estimated by integrating the area of the TPD curve, was taken as a measurement of the total acid sites concentration. Due to the poor resolution and marked broadness of the desorption profiles of some samples (especially those of aged samples), the amount of weak sites and strong sited was calculated by simply evaluating the area under the curve up to 300 °C (weak sites) and

Table 2
Acid properties of the Ce/Zr mixed oxides as a function of the calcination temperature.

Catalyst	Total acidity (μmol NH_3 g^{-1})	Strong sites (μmol NH_3 g^{-1})	Total acidity (μmol NH_3 m^{-2})	Strong sites (μmol NH_3 m^{-2})
CZ 100/0-550	187	125	1.9	1.3
CZ 80/20-550	190	88	1.9	0.9
CZ 68/32-550	198	98	2.0	1.0
CZ 50/50-550	232	126	2.3	1.3
CZ 15/85-550	249	149	2.9	1.7
CZ 0/100-550	205	113	4.0	2.2
CZ 100/0-750	87	58	1.5	1.0
CZ 80/20-750	94	52	1.8	1.0
CZ 68/32-750	108	53	1.7	0.9
CZ 50/50-750	132	69	2.0	1.0
CZ 15/85-750	145	73	2.4	1.2
CZ 0/100-750	115	67	4.4	2.6
CZ 100/0-1000	35	23	1.9	1.3
CZ 80/20-1000	40	23	3.6	2.1
CZ 68/32-1000	43	23	2.5	1.4
CZ 50/50-1000	47	25	3.1	1.7
CZ 15/85-1000	51	26	3.0	1.5
CZ 0/100-1000	54	29	5.4	2.9

above 300 °C (strong sites), respectively. These results are listed in Table 2.

In the case of the samples calcined at 550 °C, a broad desorption profile evidenced a large distribution of different types of acid sites with the presence of two distinct desorption peaks at 200 °C (weak sites) and 400 °C (strong sites). It is also notable that the intensity of desorption peaks considerably increased with the incorporation of zirconium atoms into the ceria lattice leading to a marked increase in the total and strong acidity [39]. Hence, the highest and strongest acidity was found for CZ 15/85-550. If an attempt was made to analyse the specific acid properties of mixed oxides, on the basis of the surface area, the same trend would be found with CZ 15/85-550 showing a value of 2.9 μmol NH_3 m^{-2}. Only for pure zirconia the specific acidity would be higher (4.0 μmol NH_3 m^{-2}). A recent IR study of pyridine adsorption confirmed the nature of these acid sites as Lewis sites predominantly [26]. On the other hand, it was found that the area under the TPD curves dropped significantly for all aged catalyst compared with the fresh samples, thereby showing an overall loss of the total number of acid sites with increasing calcination temperature (ranging from 50–60% at 750 °C to 80% at 1000 °C). Furthermore, the decrease in the acid character did not modify the strength distribution of the acid sites appreciably. Only a slight shift in desorption temperatures for strong sites was detected, now close to 350 °C. The observed important loss of acid sites, preferentially strong sites, was in accordance with the surface sintering (as indicated by the drop in the surface area, Table 1).

Fig. 3 shows the temperature-programmed reduction profiles for fresh and aged samples. It could be seen that fresh ceria (CZ 100/0-550) displayed a broad reduction profile with a low-temperature H_2 peak centred around 480 °C, which was related to the reduction of the uppermost layers of Ce^{4+}, and a high-temperature H_2 peak centred around 870 °C, which was originated by bulk reduction [40]. The amount of reductant involved in the process up to 650 °C is included in Table 3. On the other hand, H_2 consumption by CZ 0/100-550 (pure zirconia) was expectedly negligible since the cation Zr^{4+} was hardly reduced.

In contrast to the TPR profile for ceria, the H_2 consumption onset temperature for fresh ceria–zirconia mixed oxides was shifted to a markedly lower value (i.e., 200–250 °C for mixed oxides in comparison with 300 °C for pure ceria). Besides the reduction profiles of these samples did not present a well-defined bulk reduction peak but only a single reduction peak with a maximum located at about 550 °C with a small shoulder at higher

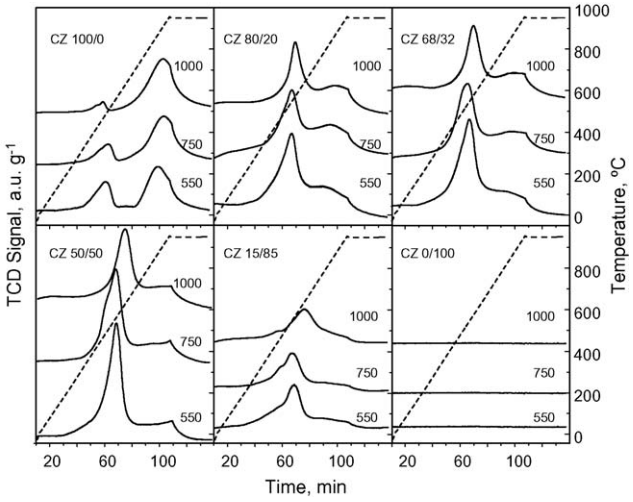

Fig. 3. H_2-TPR profiles of the Ce/Zr mixed oxides as a function of the calcination temperature.

temperature. The generally accepted argument to explain this type of profiles is that the surface and bulk reduction occurs concurrently. In other words, this peak corresponded to the reduction of the surface as well as that of some subsurface layers. Thus, insertion of ZrO_2 into the cubic CeO_2 resulted in a distortion on the mixed oxide, which allowed for a higher mobility of the lattice oxygen, and consequently reduction was no longer confined to the surface but extended deep into the bulk [41]. Since the charge/radius of Ce^{3+} (radius 1.14 Å) is significantly lower than that of Ce^{4+} (radius 0.97 Å), the formation of vacancies or structural defects was promoted, and as a consequence the oxygen mobility was favoured [42,43]. It was noted that the extent of the reduction was larger for CZ 50/50-550.

In addition to the differences observed between the reduction profiles of pure and mixed oxides, it is worth mentioning that the amount of H_2 consumed per catalyst mass by the mixed oxides was higher than that consumed by CZ 100/0-550, despite the amount of cerium was lower in the mixed samples. The values of H_2 consumption, which is a direct measurement of the amount of oxygen evolved from the sample, are useful for calculating the amount of Ce^{3+} formed during reduction ($n_{Ce^{3+}}$) [44]. Table 3 includes the values of the percentage of Ce^{3+} (%Ce^{3+}) referred to the

Table 3
Redox properties of the Ce/Zr mixed oxides as a function of the calcination temperature.

Catalyst	H_2 consumption (μmol g^{-1}) (650 °C)	Percentage of Ce^{3+} (350 °C)	Percentage of Ce^{3+} (650 °C)	Percentage of Ce^{3+} (950 °C)	% Oxygen vacancies (350 °C)	% Oxygen vacancies (650 °C)	% Oxygen vacancies (950 °C)
CZ 100/0-550	367	1.4	12.6	38.8	0.34	3.2	9.7
CZ 80/20-550	1078	3.0	43.8	69	0.58	8.8	13.8
CZ 68/32-550	1168	3.6	53.8	75	0.62	8.3	12.8
CZ 50/50-550	1212	5.1	71.6	94.6	0.64	9.0	11.8
CZ 15/85-550	588	12.7	90.1	100	0.48	3.4	3.8
CZ 0/100-550	–	–	–	–	–	–	–
CZ 100/0-750	224	0.5	7.7	35	0.13	1.9	8.8
CZ 80/20-750	668	1.3	27	51.3	0.25	5.4	10.3
CZ 68/32-750	964	1.6	44.3	72.1	0.26	7.5	12.3
CZ 50/50-750	1126	2.6	66.5	93.9	0.30	8.3	11.7
CZ 15/85-750	507	7.3	88.3	100	0.27	3.3	3.8
CZ 0/100-750	–	–	–	–	–	–	–
CZ 100/0-1000	73	0.10	2.5	33.2	2.5×10^{-2}	0.6	8.3
CZ 80/20-1000	599	0.27	24.3	47	5.4×10^{-2}	4.9	9.4
CZ 68/32-1000	652	0.33	30	55.4	5.6×10^{-2}	5.1	9.4
CZ 50/50-1000	678	0.56	40.1	72.6	7.4×10^{-2}	5.0	9.1
CZ 15/85-1000	338	1.38	58.9	100	6.3×10^{-2}	2.2	3.8
CZ 0/100-1000	–	–	–	–	–	–	–

cationic sublattice according to the following equation:

$$\%\,Ce^{3+} = \frac{n_{Ce^{3+}}}{n_{Ce_T}} \times 100 \quad (2)$$

where n_{Ce_T} is the amount of cerium ions in 1 mole of the oxide. Hence, n_{Ce_T} is equal to $(1 - x)$ if the chemical formula of the mixed oxide is written $Ce_{1-x}Zr_xO_2$. Eq. (2) can be thus rearranged as

$$n_{Ce^{3+}} = \frac{\%Ce^{3+}}{100}(1 - x) \quad (3)$$

Since the stoichiometry of the reduction process establishes that the formation of two Ce^{3+} ions corresponds to the simultaneous formation of one oxygen vacancy [36], the amount of oxygen vacancies (n_{OV}) in 1 mole of oxide can be therefore calculated as

$$n_{OV} = \frac{n_{Ce^{3+}}}{2} \quad (4)$$

The percentage of oxygen vacancies (%OV) corresponds to the percentage of vacancies present in the sample, with the anionic sublattice as a reference. This is equal to

$$\%OV = \frac{n_{OV}}{n_{OT}} \times 100 \quad (5)$$

where n_{OT} is the amount of oxygen sites in 1 mole of oxide. As n_{OT} is equal to 2 (2 moles of oxygen sites for 1 mole of oxide), Eq. (5) can be transformed into

$$\%OV = \frac{n_{OV}}{2} \times 100 \quad (6)$$

From Eqs. (3), (4) and (6) the percentage of oxygen vacancies referred to the total amount of oxygen atoms initially present in the oxide can be obtained as follows:

$$\%OV = \frac{\%Ce^{3+}}{4}(1 - x) \quad (7)$$

The %OV is an interesting parameter to discuss on the basis of the labile oxygen for the catalytic reaction since it represents how much oxygen will be available for the catalytic oxidation of the chlorinated molecules. Table 3 also lists the %OV values after the reduction process up to several reduction temperatures, namely 350, 650 and 950 °C. As a general behaviour an enhancing effect of zirconium was observed compared to the pure ceria, which was more noticeable with increasing reduction temperature.

Calcination at high temperatures (750–1000 °C) also provoked changes in the redox properties as revealed by the TPR profiles included in Fig. 3. In the case of the CZ 100/0 oxide the contribution of the first peak located at around 480 °C, attributed to the reduction of the uppermost layers of Ce^{4+}, decreased gradually as the calcination temperature was further increased. This result was in accordance with the loss of surface area observed [41,45]. As for the different mixed oxides, the decrease in H_2 consumption was less significant despite of the sintering process (ranging from 80% for CZ 100/0-1000 to 45% for CZ 50/50-1000 and 43% for CZ 15/85-1000). The fact that bulk and surface reduction occurred at the same time helped in minimising the negative effect associated with the decreased surface area (Table 1). This behaviour was more evident for Zr-rich samples. In addition, the H_2 consumption onset temperature was shifted to slightly higher temperatures (>400 °C) as a consequence of the larger crystal size when compared with the corresponding fresh sample calcined at 550 °C [46].

3.2. Catalytic performance of fresh and thermally aged Ce/Zr samples

The oxidation of 1,2-dichloroethane was chosen as a measure to assess the performance of fresh and thermally aged Ce/Zr mixed oxides. The activity of the catalysts was examined by means of the corresponding ignition or light-off curves between 200 and 250 °C, characterised by the T_{50} parameter (temperature needed to attain 50% conversion) (Table 4). As for the fresh samples a noticeable catalytic performance was observed for CZ 100/0-550 and the mixed oxide catalysts, as revealed by the low temperatures required for the deep decomposition of the chlorinated compound. In this sense, it was observed that the mixed oxide with an equimolar composition, CZ 50/50-550, showed the highest activity.

Table 4
T_{50} values (°C) of DCE and TCE oxidation over Ce/Zr mixed oxides as a function of the calcination temperature.

Catalyst	DCE			TCE		
	550 °C	750 °C	1000 °C	550 °C	750 °C	1000 °C
CZ 100/0	320	365	385	425	440	450
CZ 80/20	310	355	370	410	430	445
CZ 68/32	305	350	360	400	425	445
CZ 50/50	300	335	350	390	420	440
CZ 15/85	315	340	355	385	410	430
CZ 0/100	360	380	405	440	455	465
No catalyst		450			525	

Table 4 also includes the evolution of T_{50} values for all aged samples, submitted to calcination at 750 and 1000 °C, while Fig. 4 shows the light-off curves of two selected mixed oxides, namely CZ 50/50 and CZ 15/85 oxides. It was clearly observed that the increase in the calcination temperature led to a progressive decrease in the catalytic activity, irrespectively of the catalyst composition. However, the extent of the impact on the catalytic conversion was found to depend on the Ce/Zr ratio of the oxide. Thus, Zr-rich samples showed a lower inhibition of the catalytic activity with CZ 15/85 and CZ 50/50 showing the lowest T_{50} values. Note that these two mixed oxides were the most active under both moderate (750 °C) and severe (1000 °C) aging conditions. It was noticed that the decrease in activity evaluated in terms of the observed shift in T_{50} was more relevant when samples were calcined from 550 to 750 °C than when they calcined from 750 to 1000 °C.

DCE catalytic oxidation gave rise to CO, CO_2, HCl and Cl_2 as major oxidation products. Nevertheless, the decomposition was also accompanied by the generation of vinyl chloride (VC) up to 200 ppm between 250 and 400 °C. This by-product was presumably formed by dehydrochlorination of DCE and completely oxidised at higher temperatures [47]. Also reduced quantities (<60 ppm) of 1,1,1-trichloroethane and *cis*-1,1-dichloroethylene

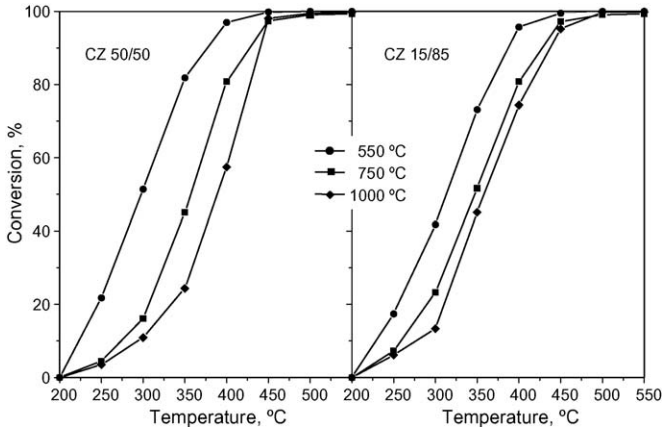

Fig. 4. Light-off curves of DCE oxidation over selected Ce/Zr mixed oxides as a function of the calcination temperature.

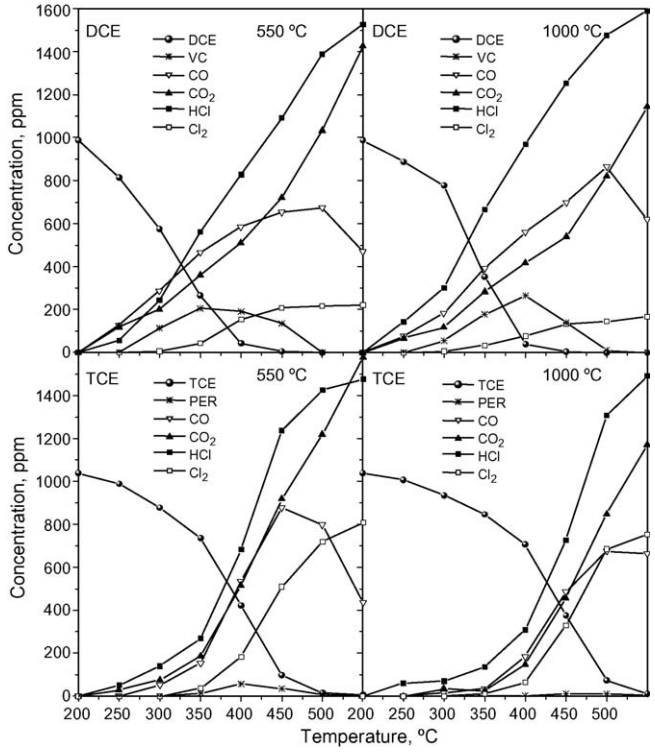

Fig. 5. Concentration profiles of the combustion of DCE and TCE over CZ 15/85 calcined at 550 and 1000 °C.

were identified. Fig. 5 compares the concentration profiles of the chlorinated feed along with the reaction products of the oxidation runs with CZ 15/85 following calcination at 550 and 1000 °C. The amount of vinyl chloride formed as an intermediate was larger for thermally aged oxides and the peak concentration was found at 400 °C in contrast to 350 °C over the fresh sample.

The formation of HCl was favoured over all investigated samples in the whole operating temperature range. Nevertheless, significant amounts of molecular chlorine were also formed. The generation of this undesired by-product depended on the Ce/Zr ratio of the mixed oxide. Hence, selectivity to Cl_2 at 550 °C increased from 4% over CZ 0/100-550 to 40% over CZ 100/0-550. On the other hand, the product spectra obtained for aged samples was comparable to that monitored for fresh samples with HCl as the predominant chlorinated reaction product as well. Interestingly, and as a general behaviour, a slight decrease in the selectivity to Cl_2 in favour of an increase in selectivity to HCl was noticed, with Cl_2 selectivity values ranging from 31–37% over CZ 50/50-550 and CZ 15/85-550 to 22–30% over the thermally aged counterparts.

Carbon dioxide was found to be the main non-chlorinated reaction product. CO was also observed in the 250–450 °C temperature range but as reaction temperature increased lower concentrations of CO were found. Hence, the CO_2 selectivity values over fresh samples were in the order of 75–95% for mixed oxides and pure ceria. The CO/CO_2 ratio was found to be the lowest for CZ 100/0-550. Conversely, pure zirconia, which is a relatively poor deep oxidation catalyst, gave rise to significant amounts of carbon monoxide with a CO_2 selectivity close to 67%. As for CO/CO_2 selectivity over thermally aged samples a significant increase in CO formation was observed. As a result, CO selectivity values ranged from 20–25% over CZ 50/50-550 and CZ 15/85-550 to 30–35% over the aged counterparts.

The behaviour of thermally aged Ce/Zr mixed oxides was also investigated for the combustion of another common chlorinated hydrocarbon, such as trichloroethylene (TCE), found in numerous waste gas streams. Fig. 4 reveals that the combustion of TCE over fresh catalysts required substantially higher reaction temperatures than DCE. Depending on the selected oxide catalyst the T_{50} values ranged from 385 to 440 °C (Table 4). These values were notably lower than the T_{50} value found in the homogeneous reaction (525 °C), thereby evidencing the active catalytic role of the investigated mixed oxides in this reaction as well. The activity pattern was similar to that noted with DCE. Thus, CZ 15/85-550 and CZ 50/50-550 exhibited the highest conversion. As in the case of DCE, mild (750 °C) and severe (1000 °C) thermal aging resulted in a significant increase in the temperatures required for oxidation. Again CZ 50/50 and CZ 15/85 showed the lowest values of T_{50} for both calcination temperatures. After heating at 1000 °C these catalysts still produced 50% conversion of TCE at 430 and 440 °C, respectively. This represents about 45–50 °C drop in reaction temperature for similar conversion level as compared with the corresponding fresh sample. By contrast, the other aged oxides needed a minimum temperature of 445 °C. It is, however, true that the differences in TCE oxidation activity among the aged samples became less noticeable with relatively close T_{50} values in contrast with the higher dispersion of the T_{50} values in DCE oxidation.

When analysing the product selectivity it was observed that the predominant oxidation products were CO_2 and HCl (Fig. 5). However, unlike DCE, chlorine gas was found in comparable concentrations to HCl. As a result, HCl selectivity values ranging from 45% (CZ 0/100-550) to 25% (CZ 100/0-550) were obtained. These values were markedly lower than those found in DCE oxidation. As expected, pure zirconia, which was characterised by a low oxidation activity, showed the highest selectivity to HCl in the combustion of the two chlorinated VOCs.

On the other hand, as was observed for the destruction of DCE over the Ce-rich oxides, the same enhancement in the CO_2 selectivity with temperature was also evident for TCE destruction. Besides, significant amounts of tetrachloroethylene (PER), 55–85 ppm, were also identified at mild temperatures (250–450 °C) as a chlorinated by-product. This compound was attributed to chlorination of TCE, and completely oxidised at higher temperatures [24]. When using aged samples as catalysts in the oxidation of this chlorinated olefin similar effects on product distribution with respect to those observed in the oxidation of DCE were noticed. Hence, Cl_2 selectivity was slightly inhibited (selectivity values ranging from 52–56% over CZ 50/50-550 and CZ 15/85-550 to 50–54% over the thermally aged counterparts) while the formation of CO was more appreciable (selectivity values ranging from 18–20% over CZ 50/50-550 and CZ 15/85-550 to 30–36% over the aged counterparts).

4. Discussion

In this work the gas-phase catalytic destruction of aliphatic chlorinated volatile organic compounds over a series of Ce/Zr mixed oxides was analysed focusing on the impact of induced thermal aging on the catalytic behaviour. A characterisation study was also undertaken to investigate the nature of the changes provoked by thermal aging in the catalytic properties. The comparative performance of fresh (calcined at 550 °C) and thermally aged (calcined at 750 and 1000 °C) samples were assessed using the oxidative destruction of 1,2-dichloroethane and trichloroethylene in a fixed flow reactor, which are two common chlorinated pollutants found in many commercial waste streams.

Considering the activity results for the fresh samples in DCE oxidation two observations could be made. Firstly, a clearly different activity was noted between pure ceria and zirconia. Hence, the former showed a T_{50} of 320 °C compared with 360 °C by the latter. Secondly, both oxides decomposed the chlorohydrocarbon at temperatures markedly lower than those required under

homogeneous conditions (in the absence of any catalyst). From characterisation results it could be established that the reaction mechanism was distinctly different. As for pure zirconia it was reasonable to expect that activity was controlled only by the surface acidity since its redox character was virtually negligible. Further evidence of the relevance of acidity in chlorocarbon destruction was previously observed for other bulk catalysts such as H-zeolites [48], TiO_2/SiO_2 [49], ZrO_2/SO_4 [50], or TiO_2/ZrO_2 [51]. On the contrary, ceria was effective for oxidising DCE due to its capability of providing active oxygen species, mainly from the surface at low temperatures.

When mixed oxides were used as catalysts, all the compositions with varying Ce/Zr ratios were appreciably more active, being CZ 50/50-550 the sample with the lowest T_{50}. As revealed by the H_2-TPR analysis, this sample presented the highest value of percentage of oxygen vacancies (9.0%) available for the oxidation reaction. In this sample both surface and bulk reduction occurred simultaneously leading to an enhancement of oxygen mobility. Further, the increased oxygen mobility with respect to the parent ceria was also evident for the other Ce/Zr mixed oxides investigated. Zr-doping decreased the onset temperature of Ce^{4+} reduction (from around 200–250 °C over the mixed oxides to about 400 °C over CZ 100/0-550), enhanced oxygen mobility within the lattice (with %OV values after reduction at 650 °C ranging from 3.4 to 9% for the mixed oxides compared with 3.2% for CZ 100/0-550) and increased the amount of Ce^{4+} that could be reduced (with $\%Ce^{3+}$ values after reduction at 650 °C ranging from 43.8 to 90.1 for the mixed oxides compared with 12.6 for CZ 100/0-550). Fig. 7 illustrates the dependence of the percentage of oxygen vacancies present in the catalytic samples after reduction up to 650 °C, which in turn was the most readily available during catalyst operation during Cl-VOC combustion, as a function of the catalyst activity in terms of T_{50}. A clear relationship could be assessed between this parameter and conversion. A particular behaviour was noticed for CZ 15/85-550 since a higher T_{50} value would be expected according to its noticeably lower value of %OV (3.4%). It only decreased by 15 °C when compared to the lowest T_{50} value exhibited by CZ 50/50-500 (300 °C) with a %OV value of 9.0%.

However, taking into account that pure zirconia was somewhat active surface acidity could also play a significant role in the reaction scheme. It is believed that acid sites can act as effective chemisorption sites for the chlorinated reactant. In fact, the key role of acidity at the catalyst surface in the activation of the organics was demonstrated in an earlier study [26]. Similarly to Fig. 7, T_{50} was plotted against the acidity of the samples in Fig. 8. In this case, the highest activity of CZ 50/50-550 could be also related to its relative large acidity. Although CZ 15/85-550 presented the largest number of acid sites (2.9 μmol NH_3 m^{-2}) among the mixed oxides, its lower percentage of oxygen vacancies (3.4%) resulted in a slightly higher reaction temperature. It is therefore reasonable to think that both catalytic properties suitably balanced for a given Ce/Zr sample lead to an optimum performance. It is also true that for DCE oxidation reducibility, that is the presence of relatively accessible lattice oxygen species at low temperatures, appears to play a more crucial role than acidity does.

Accordingly it is suggested that the first step of the oxidative process was the adsorption for the chlorinated molecule on a Lewis site (8). The adsorbed molecule could be subsequently attacked by mobile oxygen species from the solid solution through a Mars–van Krevelen mechanism. This mechanism involves two steps (9) and (10), where ≪O≫ and ≪□≫ stand for a mobile oxygen and an oxygen vacancy, respectively:

$$\mathrm{VOC\,(g)} + \ll \mathrm{acid\ site} \gg \rightarrow \mathrm{VOC_{ads}} \quad (8)$$

$$\mathrm{VOC_{ads}} + \ll \mathrm{O} \gg \rightarrow \mathrm{CO_2\,(g)} + \mathrm{H_2O\,(g)} + \mathrm{HCl\,(or\,Cl_2)\,(g)} + \ll \square \gg + \ll \mathrm{acid\ site} \gg \quad (9)$$

$$\ll \square \gg + \tfrac{1}{2}\mathrm{O_2\,(g)} \rightarrow \ll \mathrm{O} \gg \quad (10)$$

The first reaction (9) corresponds to the oxidation of the molecule involving the fast migration of oxygen species from the lattice through the lattice, and the second one (10) is the regeneration of the oxygen vacancies by adsorbed gas-phase oxygen. This mechanism was further corroborated by a series of catalytic runs carried out in the absence of oxygen in the gas stream. In these experiments the compound was oxidised but to a lower extent and, in addition, after a certain time on stream, the activity decreased. This feature was assigned to the fact that active oxygen species from the catalyst were consumed, and subsequent reoxidation by gas-phase oxygen was required to maintain a high activity [24].

After submitting the oxides to a high-temperature calcination (750 or 1000 °C), activity was negatively impacted with increasing temperature. Sintering was responsible for this behaviour since it led to an important loss of the amount of accessible catalytic sites, both redox and acid. This detrimental effect on conversion was evident for all the catalysts investigated although the decrease in activity was more or less noticeable depending on the composition. Thus, while pure ceria showed a poor thermal stability, Ce/Zr oxides exhibited a higher resistance to severe induced thermal aging [43,52]. As for %OV after reduction at 650 °C, it decreased for CZ 100/0 by 39 and 80% after calcination at 750 and 1000 °C, respectively. In contrast, this value for CZ 15/85 and CZ 50/50 only decreased by 2.1 and 9.5%, respectively, after calcination at 750 °C, and by 35 and 44% after calcination at 1000 °C, respectively. If a look is taken at Figs. 7 and 8 it is once again clearly noted that aged CZ 50/50 and CZ 15/85 were the samples that maintained the suitable combination of acid sites and oxygen vacancies that makes them exhibit the higher activity for DCE oxidation.

On the other hand, it is worth pointing out that even though samples were submitted to thermal aging at 1000 °C, the conversion achieved over all the investigated catalysts was still substantially higher than that noticed in the blank experiment (homogeneous conversion results where the catalyst was replaced by crushed quartz) with a T_{50} value of 450 °C. Although it is not very likely that the catalyst operates at temperatures as high as 1000 °C (perhaps only when the Cl-VOC is simultaneously oxidised in the presence of large amounts above 10,000 ppm of other VOCs whose highly exothermal combustion may lead to local high-

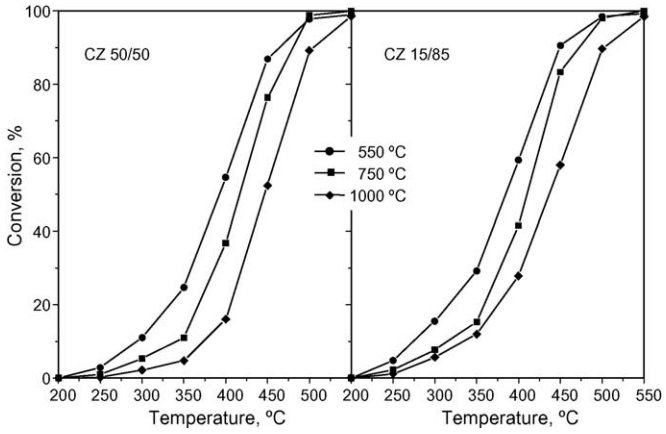

Fig. 6. Light-off curves of TCE oxidation over selected Ce/Zr mixed oxides as a function of the calcination temperature.

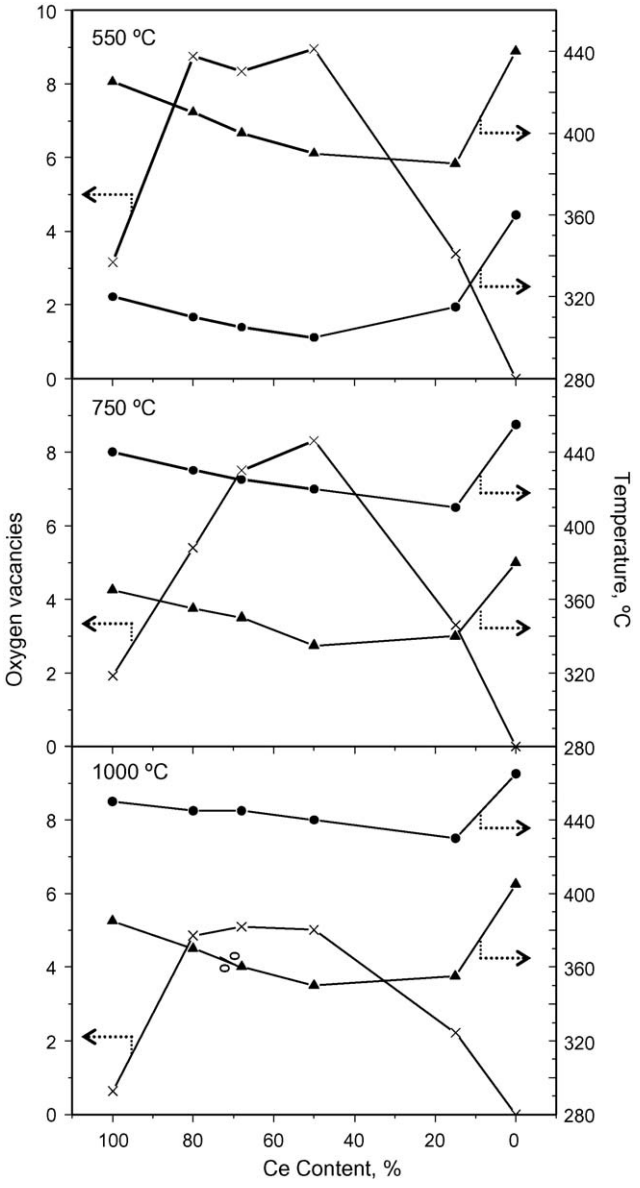

Fig. 7. Relationship between the catalytic activity (as characterised by T_{50} in DCE—triangles and TCE oxidation—circles) and the percentage of oxygen vacancies (%OV, after reduction at 650 °C) of the mixed oxides calcined at different temperatures.

temperature spots on the surface of the catalyst or when very high gas hourly space velocities are used) the results give an evidence of the remarkable activity of this type of mixed oxides and of their thermal resistance, partially preserving oxygen mobility and acidity.

Fig. 6 reveals that TCE, one of the most refractory Cl-VOC to oxidise, was decomposed at significantly higher temperatures with respect to DCE. It is widely accepted that the Cl-VOC reactivity is sensitive to the number of chlorine atoms in the molecule [32]. In this sense, Windawi and Wyatt [53] suggested that the relatively large size and high electronegativity of the chlorine atom (as opposed to the small size and low electronegativity of the hydrogen atom) could produce severe steric and electronic hindrances to the adsorption of highly chlorinated molecules. The most active catalysts were CZ 15/85-550 and CZ 50/50-550. As in the case of DCE, Figs. 7 and 8 include the relationships of the T_{50} values as a function of the %OV and acid properties, respectively. Yet again it was observed that activity was governed by an adequate combination of redox and acid sites. Unlike DCE oxidation, acidity was more crucial for activity as evidenced by the slightly better behaviour of CZ 15/85-550, the sample with the highest acidity among the mixed oxides (249 μmol NH_3 g^{-1} or 2.9 μmol NH_3 m^{-2}). It is therefore suggested that the adsorption step (8) is probably controlling the TCE oxidative reaction, with a less noticeable role of the percentage of oxygen vacancies provided that a sufficient large amount is present in the mixed oxide. Once the VOC is adsorbed, it can be oxidised by mobile oxygen entities, these being more abundant for CZ 50/50-550 with a %OV value of 8.3.

Taking together the catalytic oxidation results of the two Cl-VOCs examined (DCE and TCE) over fresh and aged samples several conclusions could be drawn. On the one hand, the oxidation of chlororganics is a demanding reaction that requires the involvement of active oxygen species from the bulk of the catalyst and an adequate surface acidity. This behaviour in contrast with the oxidation of non-chlorinated VOCs such as hexane and toluene where CZ 100/0-550 (pure ceria) showed the highest activity among all oxides evaluated, thereby suggesting the major participation of oxygen species present at the surface [54,55]. On the other hand, the higher activity exhibited by aged CZ 50/50 and CZ 15/85 mixed oxides in Cl-VOC oxidation was assigned to the

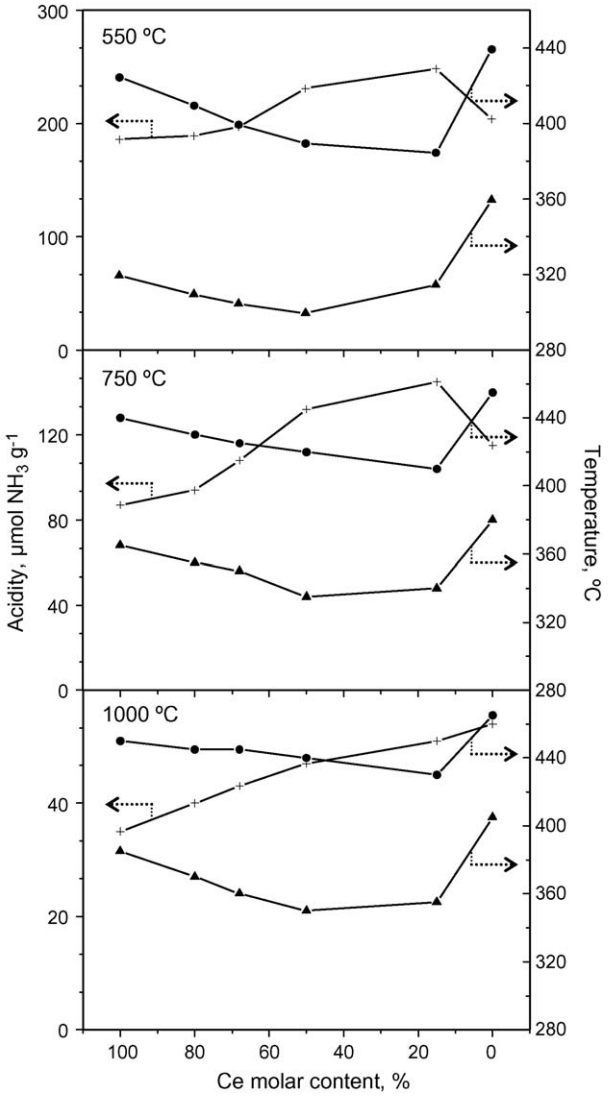

Fig. 8. Relationship between the catalytic activity (as characterised by T_{50} in DCE—triangles and TCE oxidation—circles) and the acidic properties of the mixed oxides calcined at different temperatures.

capacity of partially preserving a certain amount of acid sites (CZ 15/85) along with a marked percentage of oxygen vacancies (CZ 50/50), and a lower temperature onset for Ce^{4+} reduction (CZ 15/85).

High conversion is not the only criterion for determining good halohydrocarbon destruction catalysts. Transformation of converted carbon and chlorine atoms to carbon monoxide, chlorinated by-products and molecular chlorine, which are other toxic air pollutants, is indeed a common problem for most of catalytic systems for total oxidation of chlorinated hydrocarbons. In other words, the T_{50} criterion, which is based on the disappearance of the parent hydrocarbon, does not take into account the formation of secondary products which are sometimes much more toxic than the starting product. Consequently it is useful to provide not only curves about the disappearance of the parent molecule but also some basic information about the nature and the amount of by-products. In this way the environmental burden may be increased rather than a problem being solved.

As regards HCl/Cl_2 selectivity, two markedly different patterns were observed depending on the H/Cl ratio of the parent Cl-VOC. In DCE oxidation (H/Cl > 1) HCl formation was relatively favoured in contrast to TCE destruction where comparable amounts of both HCl and Cl_2 were generated. Not only the chemical nature did influence the product distribution but also the occurrence of the so-called Deacon reaction ($2HCl + O_2 \leftrightarrow Cl_2 + H_2O$). Furthermore, the oxidation of HCl to Cl_2 depended on the catalyst composition. Irrespective of the chlorinated compound investigated, Ce-rich mixed oxides were more selective to molecular chlorine. Note that this is important from a practical point of view since HCl can be more easily trapped and neutralised from the effluent gas stream in an alkaline medium. When using aged samples, the same qualitative behaviour could be noticed as the yield of HCl was also enhanced in DCE oxidation and for Zr-rich catalysts. Nevertheless, since the oxidation activity was limited for sintered samples the conversion of HCl into Cl_2 was somewhat inhibited. Taking into account the difficulty of molecular chlorine removal from the waste stream, previous studies have shown that performing the experiments in the presence of hydrogen-rich additives, such as water or hydrocarbons, is helpful in minimising the yield of this undesired product by reversing the Deacon reaction [54–56].

In addition to a lower catalytic activity, another negative effect associated with the decreased oxidation power of thermally aged samples was that, in line with the unfavoured formation of Cl_2 by HCl oxidation, CO oxidation to give carbon dioxide was inhibited as well. Thus, CO selectivity values ranged from 20–25% over CZ 50/50-550 and CZ 15/85-550 to 30–35% over the aged counterparts.

5. Conclusions

Better catalytic performances are achieved when ceria–zirconia solid solutions are used instead of the pure parent oxides (CeO_2 or ZrO_2). Incorporation of zirconium in the ceria lattice improves the reducibility of Ce^{4+} and the mobility of lattice oxygen. Also the acidic properties were markedly improved. On the basis of the catalytic results the activity of Ce/Zr mixed oxides could be the result of the capability of supplying oxygen which could attack the chlorinated compound previously adsorbed on acid sites. The mixed oxides with an optimum combination of both properties, $Ce_{0.5}Zr_{0.5}O_2$ and $Ce_{0.15}Zr_{0.85}O_2$, led to a higher activity for both chlorinated compounds examined. On the other hand, trichloroethylene resulted more difficult to oxidise than 1,2-dichloroethane.

Catalysts used for the oxidation of chlorinated organics were observed to be susceptible to deactivation induced by thermal sintering, since combustion temperatures were significantly increased. $Ce_{0.5}Zr_{0.5}O_2$ and $Ce_{0.15}Zr_{0.85}O_2$ demonstrated the highest resistance to deactivation with an average shift in T_{50} values of 25–35 °C (when aged at 750 °C) and 40–50 °C (when aged at 1000 °C). Calcination at high temperatures caused a negative effect on key catalytic properties (percentage of oxygen vacancies and acidity), which, in turn, was the result of sintering (decrease in surface area along with larger crystal sizes). Reaction selectivity was also affected by thermal aging since the deep oxidation ability was decreased. As a result, the yield of incomplete combustion products, namely carbon monoxide and chlorinated by-products, was relatively favoured. However, an interesting feature of deactivated samples was that they partially inhibited the formation of molecular chlorine in favour of hydrogen chloride, this is to say, the Deacon reaction was not significantly activated.

Acknowledgements

The authors wish to thank the Universidad del País Vasco/EHU-Diputación Foral de Bizkaia (DIPE06/25) for the financial support.

References

[1] R.A. Keller, J.A. Dyer, Chem. Eng. 105 (1998) 100–105.
[2] E.C. Moretti, Practical Solutions for Reducing Volatile Organic Compounds and Hazardous Air Pollutants, Center for Waste Reduction Technologies of the American Institute of Chemical Engineers, New York, 2001.
[3] S. Kawi, M. Te, Catal. Today 44 (1998) 101–109.
[4] M. Kulazynski, M.J.G. van Ommen, J. Trawczynski, J. Walendziewski, Appl. Catal. B 36 (2002) 239–247.
[5] L. Wang, M. Sakurai, H. Kameyama, J. Hazard. Mater. B 154 (2008) 390–395.
[6] P.S. Chintawar, H.L. Greene, Appl. Catal. B 13 (1997) 81–92.
[7] R. López-Fonseca, J.I. Gutiérrez-Ortiz, J.R. González-Velasco, Appl. Catal. A 271 (2004) 39–46.
[8] R.F. Howe, Appl. Catal. A 271 (2004) 3–11.
[9] A.Z. Abdullah, M.Z. Abu Bakar, S. Bhatia, J. Hazard. Mater. B 129 (2006) 39–49.
[10] G. Sinquin, C. Petit, S. Libs, J.P. Hindermann, A. Kiennemann, Appl. Catal. B 32 (2001) 37–47.
[11] E. Kantzer, D. Döbber, D. Kieβling, G. Wendt, Stud. Surf. Sci. Catal. 143 (2002) 489–497.
[12] J.I. Gutiérrez-Ortiz, B. de Rivas, R. López-Fonseca, S. Martín, J.R. González-Velasco, Chemosphere 68 (2007) 1004–1012.
[13] R.M. Lago, M.L.H. Green, C.C. Tsang, M. Odlyha, Appl. Catal. B 8 (1996) 107–121.
[14] R. Rachapudi, P.S. Chintawar, H.L. Greene, J. Catal. 185 (1999) 58–72.
[15] J. Janas, R. Janik, T. Machej, E.M. Serwicka, E. Bielanska, E. Bastardo-González, W. Jones, Catal. Today 59 (2000) 241–248.
[16] M. Guillemot, J. Mijoin, S. Mignard, P. Magnoux, Appl. Catal. A 327 (2007) 211–217.
[17] Q. Dai, X. Wang, G. Lu, Appl. Catal. B 81 (2008) 192–202.
[18] H.S. Gandhi, G.W. Graham, R.W. McCabe, J. Catal. 216 (2003) 433–442.
[19] M.V. Twigg, Appl. Catal. B 70 (2007) 2–15.
[20] B.M. Reddy, P. Lakshmanan, P. Bharali, P. Saikia, G. Thrimurthulu, M. Muhler, W. Grulnert, J. Phys. Chem. C 111 (2007) 10478–10483.
[21] S. Eriksson, S. Rojas, M. Boutonnet, J.L.G. Fierro, Appl. Catal. A 326 (2007) 8–16.
[22] D. Terribile, A. Trovarelli, C. de Leitenburg, A. Primavera, G. Dolcetti, Catal. Today 47 (1999) 133–140.
[23] I. Atribak, A. Bueno-López, A. García-García, J. Catal. 259 (2008) 123–132.
[24] J.I. Gutiérrez-Ortiz, B. de Rivas, R. López-Fonseca, J.R. González-Velasco, Appl. Catal. A 269 (2004) 147–155.
[25] E. Díaz, B. de Rivas, R. López-Fonseca, S. Ordóñez, J.I. Gutiérrez-Ortiz, J. Chromatogr. A 1116 (2006) 230–239.
[26] B. de Rivas, R. López-Fonseca, J.R. González-Velasco, J.I. Gutiérrez-Ortiz, J. Mol. Catal. A 278 (2007) 181–188.
[27] S. Chatterjee, H.L. Greene, J. Park, Catal. Today 11 (1992) 569–596.
[28] R. López-Fonseca, A. Aranzabal, P. Steltenpohl, J.I. Gutiérrez-Ortiz, J.R. González-Velasco, Catal. Today 62 (2000) 367–377.
[29] E. Finocchio, C. Pistarino, S. Dellepiane, B. Serra, S. Braggio, M. Baldi, G. Busca, Catal. Today 75 (2002) 263–267.
[30] C.E. Hetrick, J. Lichtenberger, M.D. Amiridis, Appl. Catal. B 77 (2008) 255–263.
[31] B. de Rivas, R. López-Fonseca, M.A. Gutiérrez-Ortiz, J.I. Gutiérrez-Ortiz, in: M. Zamorano, C.A. Brebbia, A.G. Kungolos, V. Popov, H. Itoh (Eds.), WIT Transactions on Ecology and the Environment (vol. 109, Waste Management and the Environment IV), WIT Press, Southampton, 2008, pp. 857–866.
[32] R. López-Fonseca, J.I. Gutiérrez-Ortiz, M.A. Gutiérrez-Ortiz, J.R. González-Velasco, J. Chem. Technol. Biotechnol. 78 (2003) 15–22.
[33] C. Bozo, F. Gaillard, N. Guilhaume, Appl. Catal. A 220 (2001) 69–77.
[34] K. Hashimoto, N. Toukai, R. Hamada, S. Imamura, Catal. Lett. 50 (1998) 193–198.
[35] M. Ozawa, J. Alloys Compd. 1090 (2006) 408–412.
[36] A. Trovarelli, Catalysis by Ceria and Related Materials, Catalytic Science Series, vol.2, Imperial College Press, London, 2002.
[37] G. Colón, F. Valdivieso, M. Pijolat, R.T. Baker, J.J. Calvino, S. Bernal, Catal. Today 50 (1999) 271–284.

[38] S. Yao-Matsuo, S. Otsuka, T. Yao, T. Omata, High Temp. Mater. Process. 22 (2003) 157–164.
[39] G. Ranga Rao, T. Rajkumar, J. Colloid Interface Sci. 324 (2008) 134–141.
[40] F. Giordano, A. Trovarelli, C. de Leitenburg, M. Giona, J. Catal. 193 (2000) 273–282.
[41] M. Boaro, M. Vicario, C. de Leitenburg, G. Dolcetti, A. Trovarelli, Catal. Today 77 (2003) 407–417.
[42] G. Balducci, J. Kaspar, P. Fornasiero, M. Graziani, J. Phys. Chem. B 101 (1997) 1750–1753.
[43] A.E. Nelson, K.H. Schulz, Appl. Surf. Sci. 210 (2003) 206–221.
[44] A.I. Kozlov, D.H. Kim, A. Yezerets, P. Andersen, H.H. Kung, M.C. Kung, J. Catal. 209 (2002) 417–426.
[45] S. Damyanova, B. Pawelec, K. Arishtirova, M.V. Martínez-Huerta, J.L.G. Fierro, Appl. Catal. A 337 (2008) 86–96.
[46] T. Bunluesin, R.J. Gorte, G.W. Graham, Appl. Catal. B 15 (1998) 107–114.
[47] K. Ramanathan, J.J. Spivey, Combust. Sci. Technol. 63 (1989) 247–255.
[48] R. López-Fonseca, J.I. Gutiérrez-Ortiz, M.A. Gutiérrez-Ortiz, J.R. González-Velasco, Recent Res. Dev. Catal. 2 (2003) 51–75.
[49] T. Liu, T.I. Cheng, Catal. Today 26 (1995) 71–77.
[50] W.B. Feaver, J.A. Rossin, Catal. Today 54 (1999) 13–22.
[51] M. Tajima, M. Niwa, Y. Fuji, Y. Koinuma, R. Aizawa, S. Kushiyama, S. Kobayashi, K. Mizuno, H. Ohuchi, Appl. Catal. B 12 (1997) 263–276.
[52] C. Bozo, N. Guilhaume, E. Garbowski, M. Primet, Catal. Today 59 (2000) 33–45.
[53] H. Windawi, M. Wyatt, Platinum Met. Rev. 37 (1993) 186–193.
[54] B. de Rivas, J.I. Gutiérrez-Ortiz, R. López-Fonseca, J.R. González-Velasco, Appl. Catal. A 314 (2006) 54–63.
[55] J.I. Gutiérrez-Ortiz, B. de Rivas, R. López-Fonseca, J.R. González-Velasco, Appl. Catal. B 65 (2006) 191–200.
[56] R. López-Fonseca, S. Cibrián, J.I. Gutiérrez-Ortiz, M.A. Gutiérrez-Ortiz, J.R. González-Velasco, AIChE J. 49 (2003) 496–504.